Sandia National Laboratories
Waste Isolation Pilot Plant

Actinide(IV)-Humic Complexation in the WIPP Performance Assessment

Work carried out under the Analysis Plan for the Evaluation of
Humic-Actinide Complexation for WIPP Conditions, AP 167, Rev. 0.
To be included in the AP-167 records package

Author: _____ 10-13-16
Paul E. Mariner, Org. 06224   Date

Technical Reviewer: _____ 10-13-16
Sungtae Kim, Org. 06931   Date

QA Reviewer: _____ 10-13-16
Shelly R. Nielsen, Org. 06930   Date

Management Reviewer: _____ 10-13-16
Christi D. Leigh, Org. 06932   Date
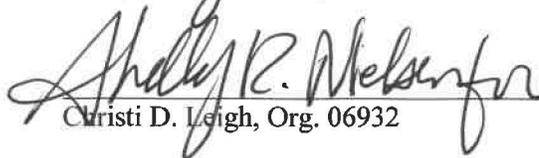
WIPP:4.4.2.2.1:PA:QA-L:567221

1

This page intentionally left blank

Actinide(IV)-Humic Complexation in the WIPP Performance Assessment

Paul E. Mariner

Sandia National Laboratories
P.O. Box 5800
Albuquerque, New Mexico 87185-MS0747

Abstract

The legacy humic colloid model for tetravalent actinides (Th(IV), U(IV), Np(IV), and Pu(IV)) in the performance assessment (PA) of the Waste Isolation Pilot Plant (WIPP) is highly conservative. The model structure is feasible, but substantial reductions are needed for two coefficients, PHUMSIM and PHUMCIM. These proportionality coefficients represent the equilibrium aqueous concentration ratio of humic-bound actinide to non-colloidal actinide for the brines of the Salado and Castile formations. In the WIPP PA model, PHUMSIM and PHUMCIM are set at 6.3 based on a conservative upper bound determined from observed colloidal partitioning of Th(IV) in seawater. This value greatly enhances the mobility of An(IV) in the WIPP PA. Actual humic partitioning of An(IV) in WIPP brines is expected to be significantly lower because the pH of brines in the WIPP environment is higher (~9), concentrations of competing cations (e.g., Mg^{2+}) are higher, and concentrations of aqueous humic substances are likely lower. In this work, the results of recent studies of An(IV)-humic and Ca^{2+}-humic complexation are used to simulate competitive humic complexation for the WIPP PA and to estimate new An(IV) PHUMSIM and PHUMCIM values. The new distributions have ranges of 0.0001 to 0.01 and 0.004 to 0.1, respectively. These distributions, which are arguably conservative, reduce humic-bound An(IV) to no more than 10% of total mobile An(IV) concentrations and reduce the total mobile An(IV) concentrations by 85% to 86% if no other types of An(IV) colloids (i.e., intrinsic, microbial, and mineral fragment colloids) are present in significant concentrations.

This page intentionally left blank

4

CONTENTS

5

FIGURES

6

TABLES

NOMENCLATURE

AHA	Aldrich humic acid
An	Actinide
An(IV)	Tetravalent actinide
AnHS	Actinide-humic site complex
AP	Analysis plan
BCHA	Belgian Boom clay humic acid
CFR	Code of Federal Regulations
DBR	Direct brine release
DOE	U.S. Department of Energy
EDTA	Ethylenediaminetetraacetic acid
EHA	Elliot soil humic acid
Eq.	Equation
ERDA-6	Energy Research and Develop Administration WIPP Well 6
GWB	Generic Weep Brine
M	Molarity
MgO	Magnesium oxide
NM	New Mexico
PA	Performance Assessment
pcH	Negative log of the calculated molar concentration of hydrogen ion
pH	Negative log of the hydrogen ion activity
PHA	Pahokee peat humic acid
PHUMCIM	Proportionality coefficient for concentration of actinides associated with mobile humic colloids in Castile brine
PHUMSIM	Proportionality coefficient for concentration of actinides associated with mobile humic colloids in Salado brine
SNL	Sandia National Laboratories
WIPP	Waste Isolation Pilot Plant

8

1 INTRODUCTION

In the current performance assessment (PA) of the Waste Isolation Pilot Plant (WIPP), humic colloids are significant contributors to the mobility of tetravalent actinides (i.e., Pu(IV), Th(IV), Np(IV), and U(IV)) (DOE 2009, SOTERM-4.7). At the time the original humic colloid model was developed for the WIPP PA, there were few published humic complexation data for tetravalent actinides (An(IV)) in saline, alkaline waters. Consequently, An(IV)-humic complexation in the WIPP PA model was based on a study by Baskaran et al. (1992) that reported colloidal and non-colloidal Th(IV) concentrations in seawater (DOE 1996, SOTERM.6.3.3.1). A summary of the study is provided in Mariner and Sassani (2014, 5.3.4.4). Assuming analogous behavior in WIPP brines and a humic colloid concentration of 2 mg L^{-1}, a proportionality coefficient of 6.3 was adopted for the ratio of humic-bound aqueous actinide concentration (AnHs) to non-colloidal aqueous actinide concentration (An). This coefficient in the WIPP PA is known as PHUMSIM for Salado formation brine and PHUMCIM for Castile formation brine.

The 6.3 proportionality coefficient is likely highly conservative. For one, aqueous humic substances may be unstable under nominal WIPP conditions in which brines are equilibrated with MgO, a chemical buffer emplaced with the waste (Wall and Mathews 2005); thus, the 2 mg L^{-1} humic colloid concentration conservatively assumed for WIPP brines may be much too high for nominal conditions. The 2 mg L^{-1} concentration used in the WIPP PA model is based on the maximum range of concentrations observed in humic solubility experiments performed on NaCl brine solutions containing Ca^{2+} and Mg^{2+} at concentrations ranging from 10 to 500 mM (DOE 1996, SOTERM.6.3.3.1). The assumed 2 mg L^{-1} concentration is likely more appropriate for a short-term borehole intrusion scenario where brine from a pressurized zone that is not equilibrated with MgO flows through the borehole and into the repository. As humic colloid concentration increases, the predicted fraction of mobile An(IV) bound to humic colloids increases (Reiller et al. 2003, Fig. 8). Second, whereas the pH of seawater is around 8, the pH of brines in the repository is predicted to be around 9 (Domski and Xiong 2015). Increases in pH in the alkaline range significantly reduce overall An(IV)-humic complexation (e.g., Reiller et al. 2003, Fig. 8). Third, Mg^{2+} from MgO will compete strongly with released actinides for humic complexation sites and limit the concentrations of humic-bound An(IV). Aqueous Mg^{2+} concentrations in WIPP brines equilibrated with MgO are expected to be 3 to 11 times higher than in seawater (Mariner and Sassani 2014, 5.3.4.4).

Since the mid-1990s when the original humic colloids model was developed for the WIPP PA, a number of studies of An(IV)-humic complexation have been published (Reiller et al. 2003; Warwick et al. 2005; Gaona et al. 2008; Reiller et al. 2008; Evans et al. 2011; Stern et al. 2014; Zimmerman et al. 2014). These studies examine complexation over a broad pH range and include laboratory measurements of humic complexation with Th(IV), Pu(IV), and U(IV). In addition, studies of the humic complexation of Ca^{2+} and Mg^{2+} over broad ranges of pH and salinity have been published (Lead et al. 1994; Laszak and Choppin 2001; Lu and Allen 2002). These studies were used in this work to build an An(IV)-humic complexation model to calculate new An(IV) PHUMSIM and PHUMCIM values for WIPP conditions.

This report is completed under the Analysis Plan for the Evaluation of Humic-Actinide Complexation for WIPP Conditions, AP 167, Rev. 0 (Mariner 2014). This report partially fulfills the scope of AP 167 in that all four tasks were completed for An(IV)-humic complexation and not for humic complexation with actinides of other redox valences (III, V, and VI).

2 HUMIC SUBSTANCES

Aqueous humic substances are a mixture of humic and fulvic acids. Humic acid by definition is soluble only below pH 10. Fulvic acid is soluble at all pH values.

The structure of humic substances is far from uniform. The range of molecular weight of humic molecules that make up the aqueous humic fraction vary over three orders of magnitude up to approximately 100,000 atomic mass units. A typical humic macromolecule contains aromatic rings and aliphatic chains that host numerous carboxylic, hydroxyl, and other functional groups. Other characteristics are the presence of nitrogen groups, a highly polyelectrolyte nature, and inter-/intra-molecular aggregation (Buffle 1988).

In natural waters, humic substances originate from the decomposition of plant and animal tissues and residues. At the WIPP, they may largely be a product of biotic or abiotic degradation of emplaced organic materials. The WIPP humic colloid model assumes that humic colloids are present at a concentration of 2 mg L^{-1} in WIPP brines (Section 3).

The aqueous stability of humic colloids is controlled by the solution composition and primarily by the cation concentrations and the solution pH. At higher ionic strength, the rates of aggregation and flocculation tend to increase, reducing stability. Wall and Mathews (2005) show that for WIPP brines in the presence of MgO, concentrations of humic colloids fall below detection within a matter of weeks. The detection limit in the Wall and Mathews (2005) study appears to be around 1 to 2 mg L^{-1} based on the error bars on the plotted data. However, without definitive evidence that humic colloid concentrations are much lower than 2 mg L^{-1} in WIPP brines in the presence of MgO, the calculations in this study will continue to assume that humic colloids are present at a concentration of 2 mg L^{-1} in WIPP brines.

Humic colloids are potentially important to the WIPP PA because they increase the concentrations of actinides in solution. Carboxylic and phenolic functional groups on humic substances act to chelate cations. Positively-charged actinides such as Th^{4+}, U^{4+}, Pu^{4+}, and Np^{4+} have a strong affinity for these functional groups. Thus, by providing additional aqueous complexation sites, humic colloids can increase the aqueous concentrations of actinides. Section 4 further addresses humic complexation of actinides and alkaline earth metals.

Humic colloids are assumed not to adsorb in the WIPP PA. Adsorption of humic colloids to stationary geologic media retards aqueous transport and can reduce concentrations. Physical and chemical mechanisms are postulated to describe adsorption of humic substances. The principle physical mechanism for adsorption of humic substances is that the solid-liquid interface provides a state of lower energy for humic molecules resulting from the hydrophobic nature of various humic components. The chemical mechanism involves inner-sphere complexation of humic functional groups with mineral surface hydroxyl groups. Humic substances adsorb readily to the net positively charged surfaces of aluminum oxide clays and adsorb little to negatively-charged silica surfaces (Buffle 1988).

Should humic colloids not interact with geologic media, they have the potential for facilitated transport, i.e., mean velocities greater than the velocity of the average water molecule (Enfield et al. 1989). The possibility of facilitated transport of actinides bound to colloids is not pursued in the WIPP PA, however, mainly because the direct brine release (DBR) scenario bypasses the porous media and deposits all releases on the ground surface.

Information Only

3   WIPP ENVIRONMENT

The compositions of groundwater in the Salado and Castile formations are represented in the WIPP PA by GWB (Generic Weep Brine) and ERDA-6 (Energy Research and Develop Administration WIPP Well 6). The compositions of these brines after equilibration with halite (NaCl), anhydrite ($CaSO_4$), hydromagnesite ($Mg_5(CO_3)_4(OH)_2 \cdot 4H_2O$), and brucite ($Mg(OH)_2$) are shown in Table 1 for the minimum volume of brine ($1 \times Min$) required for a DBR from the repository and for five times the minimum volume ($5 \times Min$) (Domski and Xiong 2015). These volumes are conservatively assumed to contain the expected inventory of acetate, citrate, ethylenediaminetetraacetic acid (EDTA), and oxalate (Domski and Xiong 2015).

Metal corrosion within the WIPP repository may serve to maintain reducing conditions. The kinetics of corrosion reactions will be controlled by the availability of H_2O at the metal surface. The predominant metals will be iron (Fe) in the form of low-carbon steel and chemical-grade lead (Pb). These metals are present within the waste itself, as well as in the containers used to hold the waste during emplacement.

In addition to the organic acids, Fe, and Pb, the waste disposed at the WIPP contains significant quantities of cellulosic, plastic and rubber materials. With time, microbial activity and abiotic reactions may consume a portion of these organic materials, resulting in the generation of carbon dioxide (CO_2), hydrogen sulfide (H_2S), hydrogen (H_2), nitrogen (N_2), methane (CH_4), and humic substances.

In the WIPP PA brines, the ionic strength is around 6 M, much higher than the ionic strength in most humic complexation studies. Such high ionic strength and high concentrations of Mg^{2+} may destabilize humic colloids in the aqueous phase (Wall and Mathews 2005). However, as in the original WIPP humic colloids model, the concentration of humic substances in the Salado and Castile brines is assumed to be 2.0 mg L^{-1}. This concentration was adopted based on the solubility range observed in systems containing Ca^{2+} and Mg^{2+} at concentrations of at least 0.01 M (DOE 1996, SOTERM.6.3.3.1). This concentration is expected to be conservative.

The site binding capacities of humic substances for the WIPP PA were estimated from experiments using Lake Bradford humic acid, Gorleben humic acid, and Suwannee River fulvic acid (DOE 1996, SOTERM.6.3.3.1). The experiments involved NaCl solutions of 3 and 6 molal, and fixed pH values of either 4.8 or 6. The site binding capacities were determined to be 4.65, 5.38, and 5.56 meq g^{-1}, respectively. Multiplying these values by the humic colloid concentration gives the following values for the total humic complexation site concentration (Hs_{tot}): 9.3×10^{-6} M, 1.1×10^{-5} M, and 1.1×10^{-5} M. The concentration of humic colloid complexation sites adopted in the present work is 1.1×10^{-5} M.

Table 1. Predicted compositions of GWB and ERDA-6 in the minimum volume (1 × Min) and five times the minimum volume (5 × Min) of brine required for a DBR from the repository (Domski and Xiong 2015)

Element or Property	Units	GWB (1 × Min[a])	GWB (5 × Min)	ERDA-6 (1 × Min)	ERDA-6 (5 × Min)
B(III) (aq)	M	0.167	0.168	0.0622	0.0623
Na(I) (aq)	M	4.70	4.71	5.38	5.40
Mg(II) (aq)	M	0.518	0.498	0.134	0.113
K(I) (aq)	M	0.531	0.530	0.0958	0.0959
Ca(II) (aq)	M	0.0213	0.0214	0.0134	0.0126
S(VI) (aq)	M	0.220	0.209	0.181	0.171
Cl(-I) (aq)	M	5.65	5.68	5.31	5.33
Br(-I) (aq)	M	0.0302	0.0302	0.0109	0.0109
CO_2 fugacity	atm	5.84×10^{-7}	5.84×10^{-7}	5.84×10^{-7}	5.84×10^{-7}
Ionic strength	M	6.08	6.08	5.80	5.79
pcH[b]	-log(M)	9.59	9.60	9.94	9.98
pH[c]	-log(M)	8.84	8.84	9.22	9.26
Total inorganic carbon	M	0.0694	0.0142	0.0603	0.0123
Acetate	M	2.30×10^{-2}	4.61×10^{-3}	2.30×10^{-2}	4.61×10^{-3}
Citrate	M	2.33×10^{-3}	4.65×10^{-4}	2.33×10^{-3}	4.65×10^{-4}
EDTA	M	7.40×10^{-5}	1.48×10^{-5}	7.40×10^{-5}	1.48×10^{-5}
Oxalate	M	1.18×10^{-2}	2.36×10^{-3}	1.18×10^{-2}	2.36×10^{-3}
Th(IV)	M	4.78×10^{-8}	4.80×10^{-8}	5.46×10^{-8}	5.54×10^{-8}
Th^{4+}	M	1.16×10^{-25}	1.03×10^{-25}	1.12×10^{-26}	7.28×10^{-27}
Activity coefficient of Th^{4+} [d]	-	$10^{0.2696}$	$10^{0.3169}$	$10^{-0.2558}$	$10^{-0.2231}$
Activity of water [d]	-	0.73358	0.73416	0.74787	0.74844
Solution density [d]	g mL^{-1}	1.2458	1.2446	1.2218	1.2204
Ca^{2+} [d]	molal	0.0225	0.0232	0.0131	0.0131
Mg^{2+} [d]	molal	0.226	0.222	0.0414	0.0343

[a] Min = minimum brine volume for a DBR from the repository (17,400 m^3)

[b] Negative log of the hydrogen ion concentration (M)

[c] Negative log of the hydrogen ion activity (M) on the Pitzer scale

[d] From gwb_1x.6o, gwb_5x.6o, erda_1x.6o, and erda_5x.6o EQ6 output files of Domski and Xiong (2015)

4 METAL-HUMIC COMPLEXATION MODEL

A computational model was developed to simulate An(IV)-humic complexation under WIPP conditions. Section 4.1 describes the mathematical model. It differs slightly from the original WIPP humic colloid model for actinides of the III, V, and VI oxidation states. Section 4.2 presents the thermodynamic data used for the model and describes how the humic complexation stability constants were selected or derived. Humic-complexation data are presented for H^+, Ca^{2+}, and Mg^{2+} (Section 4.2.1), Th(IV) (Section 4.2.2), U(IV) (Section 4.2.3), and Pu(IV) (Section 4.2.4).

Computation of the mathematical model is facilitated at low ionic strength in this report using PhreeqcI (version 2.12.5-669), a code developed at the U.S. Geological Survey for chemical speciation, batch reaction, and one-dimensional reactive transport (Parkhurst 1995; Parkhurst and Appelo 1999; USGS 2002; USGS 2005). PhreeqcI is used in Sections 4.2.2 and 5.1 to simulate subsets of the Th(IV)-humic-Ca-Mg-EDTA-CO_2-H_2O system. The database used in the PhreeqcI calculations is the YMP_R2.dat database that comes with the PhreeqcI version 2.12.5-669 software package; however, all of the reactions that produce aqueous species that are relevant to this analysis are entered into the PhreeqcI input files to ensure quality control of thermodynamic data. Final PhreeqcI calculations were executed by Paul Domski on a qualified installation on a personal computer with Intel® Xeon™ CPU 2.27GHz (S923775) and Microsoft Windows 7 Enterprise (service pack 1).

EQ3/6 version 8.0a, not PhreeqcI, was planned for this analysis (Mariner 2014). PhreeqcI was used instead of EQ3/6 largely because PhreeqcI has more flexibility in its ion activity models for handling humic species. In addition, unlike EQ3/6, PhreeqcI allows modification and addition of reactions and equilibrium constants within the input file, which is convenient for many of the tasks involved in this analysis and provides a more straightforward means for tracing and reproducing the calculations. All calculations in this report are stored on the CVS (Concurrent Versioning System) in /nfs/data/CVSLIB/WIPP_EXTERNAL/ap167/Files.

4.1 Model Equations

The WIPP humic colloids model calculates the aqueous humic-bound actinide concentration (AnHs) from the non-colloidal aqueous concentration (An) and a proportionality coefficient H:

$$(AnHs) = H(An) \qquad \text{(Eq. 1)}$$

The proportionality coefficient H is called PHUMSIM or PHUMCIM in the PA (DOE 1996, SOTERM.6.3.3). PHUMSIM is used for the Salado brine, represented by GWB, and PHUMCIM is used for the Castile brine, represented by ERDA-6. To calculate the "mobile" actinide concentration in the PA, (AnHs) is added to (An) along with the concentrations of actinides associated with other colloids (intrinsic, microbial, and mineral fragment).

A conservative assumption of the WIPP PA is that (An) in the DBR scenario is at chemical saturation with respect to a controlling mineral phase. Thus, (An) is the calculated solubility of the actinide in WIPP brines in the presence of MgO and organic acid wastes, excluding colloids. EQ3/6 (Wolery and Jarek 2003) and the DATA0.FM2 Pitzer ion interaction database (Domski 2015) were used to calculate (An) for each brine (Domski and Xiong 2015). Calculated (An) can vary broadly among realizations due to the broad ranges of actinide solubility measurements reported in the literature.

In this work, new values for PHUMSIM and PHUMCIM for An(IV) are calculated using a traditional model for humic complexation and recent data from the literature. In this model, actinide-humic complexation is described by the reaction

$$An^{m+} + Hs^- \Leftrightarrow AnHs \qquad \text{(Eq. 2)}$$

where An^{m+} is the free actinide species (e.g., Th^{4+}) and Hs^- is an available humic substance complexation site. The conditional stability constant ($\beta_{1:An^{m+}}$) for this reaction is represented by

$$\beta_{1:An+} = \frac{(AnHs)}{(An^{m+})(Hs^-)} \qquad \text{(Eq. 3)}$$

Only 1:1 binding of An^{m+} and Hs^- is assumed to occur. This treatment of the reaction does not conserve charge and assumes homogeneous complexation sites with no acido-basic properties; however, this approach is acceptable when stability parameters such as $\beta_{1:An^{m+}}$ are conditional (Reiller et al. 2008). This treatment is nearly the same as the model used in the original WIPP model for actinides at the III, V, and VI oxidation states. The main difference is that the model defined here uses the free ion actinide concentration (An^{m+}) as the reactant instead of the aqueous non-colloidal actinide concentration (An).

Ca^{2+} and Mg^{2+} are abundant in WIPP brines and compete with actinides for humic complexation sites. The WIPP colloid model for actinides at the III, V, and VI oxidation states accounts for this effect by including terms for humic-bound Ca^{2+} and Mg^{2+} in the calculation of (Hs^-) (DOE 1996, Eq. 6-20). A similar approach is used here to account for competition by Ca^{2+} and Mg^{2+} except, as in the case of actinide-humic complexation above, free ion concentrations are used as reactants instead of aqueous non-colloidal concentrations. The concentration of available humic complexation sites is calculated from

$$(Hs^-) = \frac{(Hs_{tot})}{\beta_{1:An^{m+}}(An^{m+}) + \beta_{1:Ca^{2+}}\left((Ca^{2+}) + (Mg^{2+})\right) + 1} \qquad \text{(Eq. 4)}$$

where $\beta_{1:Ca^{2+}}$ is the stability constant for Ca^{2+}-humic complexation (used also for Mg^{2+}-humic complexation) and (Hs_{tot}) is the total concentration of aqueous humic complexation sites.

The concentration of AnHs is calculated by solving Eq. 3 for (Hs^-), substituting the result into Eq. 4, and solving for (AnHs). This gives the following expression for (AnHs):

$$(AnHs) = \frac{\beta_{1:An^{m+}}(An^{m+})(Hs_{tot})}{\beta_{1:An^{m+}}(An^{m+}) + \beta_{1:Ca^{2+}}\left((Ca^{2+}) + (Mg^{2+})\right) + 1} \qquad \text{(Eq. 5)}$$

With appropriate values for free ion concentrations and stability constants, PHUMSIM and PHUMCIM can be calculated from Eq. 5 and Eq. 1.

4.2 Model Reactions

Two sets of chemical reaction databases are used in the computational model. One is a set of intrinsic aqueous reactions with log K values, and the other is a set of humic complexation reactions with log β values. Recall that K is an equilibrium *activity* quotient, and β is an equilibrium *concentration* quotient at the specified ionic strength. The corresponding databases used in this study are shown in Table 2 and Table 3.

Table 2 gives the reactions of the Th-Ca-Mg-EDTA-CO_2-H_2O system for modeling WIPP brines in the absence of humic colloids. The first column of data lists the log β values provided in Stern et al. (2014) at 0.1 M ionic strength. EDTA is included in this table because it is a component in the Stern et al. (2014) laboratory experiments and is assumed to be prevalent in WIPP PA brines (Domski and Xiong 2015). The second column of data shows the WIPP PA DATA0.FM2 database log K values at infinite dilution (0 M) (Domski 2015). These log K values are used in the input files cited in Sections 4.2.2 and 5 (Table 4 and Table 7). The log β values in the last column are the concentration quotients corresponding to the DATA0.FM2 log K values at 0.1 M ionic strength. These latter values are calculated by PhreeqcI using the Davies equation and are documented in the input/output files of Sections 4.2.2 and 5 (Table 4 and Table 7). They are shown in this table so that they may be compared to the Stern et al. (2014) log β values and the intrinsic log K values. The Davies equation calculates activity coefficients as a function of ionic strength and species charge. Above 0.1 M ionic strength, specific ion interactions become important and the accuracy of the Davies equation deteriorates.

Table 3 shows the humic complexation reactions simulated in the PhreeqcI calculations. The first column of data shows the log β values taken from the literature. These values are conditional to an ionic strength of 0.1 M and are appropriate for the set of reactions used in the source studies. Each of these values is taken from data on humic acid. The affinity for complexation of cations is typically significantly stronger for humic acids than for fulvic acids. The log K values at infinite dilution (0 M) achieve the same partitioning observed in the source studies when the DATA0.FM2 database in Table 2 is used. The final column shows the corresponding log β values at 0.1 M ionic strength, as calculated by PhreeqcI and the Davies equation.

The selection of the log β values and the derivation of the log K values are described in Sections 4.2.1 and 4.2.2. The Davies equation is used to calculate the activity coefficients for Th^{4+}, Mg^{2+}, and Ca^{2+} in the PhreeqcI simulations. Because concentrations and concentration ratios are typically reported in metal-humic complexation studies, the activity coefficients of all humic species defined in the PhreeqcI model are fixed at a value of one. This is done by entering "`-gamma 1e6 0.0`" where these species are defined.

Table 2. Th(IV)-Ca-Mg-EDTA-CO$_2$-H$_2$O reaction database

Reaction	Log β (0.1 M) (Stern et al. 2014)	Log K (0 M) DATA0.FM2 (Domski 2015)	Log β (0.1 M)[e] for DATA0.FM2
$H_2O = OH^- + H^+$	nr[a]	-13.9967	-13.8
$HCO_3^- = CO_3^{2-} + H^+$	nr	-10.3392	-10.0
$HCO_3^- + H^+ = CO_2(aq) + H_2O$	nr	6.3374	6.22
$HCO_3^- + H^+ = CO_2(g) + H_2O$	nr	7.8193	7.71
$Th^{4+} + 4\ H_2O = Th(OH)_4(aq) + 4\ H^+$	-18.3	-17.5002	-19.2
$Th^{4+} + 3\ H_2O = Th(OH)_3^+ + 3\ H^+$	-12.7	na[b]	na
$Th^{4+} + 2\ H_2O = Th(OH)_2^{2+} + 2\ H^+$	-7.7	na	na
$Th^{4+} + H_2O = ThOH^{3+} + H^+$	-2.8	na	na
$H^+ + Edta^{4-} = HEdta^{3-}$	10.24	10.5707	9.82
$2\ H^+ + Edta^{4-} = H_2Edta^{2-}$	16.25	17.4500	16.2
$3\ H^+ + Edta^{4-} = H_3Edta^-$	19.05	20.5374	18.9
$4\ H^+ + Edta^{4-} = H_4Edta(aq)$	21.54	23.0393	21.3
$Th^{4+} + Edta^{4-} = ThEdta(aq)$	23.19	23.5570	20.1
$Th^{4+} + HEdta^{3-} = ThHEdta^+$	17.00	na	na
$Ca^{2+} + Edta^{4-} = CaEdta^{2-}$	nr	11.1562	9.48
$Mg^{2+} + Edta^{4-} = MgEdta^{2-}$	nr	10.1260	8.50
$Th^{4+} + CO_2(g) + 4\ H_2O = Th(OH)_3CO_3^- + 5\ H^+$	-20.36[c]	-21.8650[d]	-23.5
$Th^{4+} + 5\ HCO_3^- = Th(CO_3)_5^{6-} + 5\ H^+$	nr	-24.5828	-23.0
$Mg^{2+} + HCO_3^- = MgCO_3(aq) + H^+$	nr	-7.4108	-7.87
$Ca^{2+} + HCO_3^- = CaCO_3(aq) + H^+$	nr	-7.1880	-7.70

[a] nr = not reported; [b] na = not applicable to DATA0.FM2 database; [c] see text in step 1 of Section 4.2.2; [d] Calculated from $Th^{4+} + HCO_3^- + 3\ H_2O = Th(OH)_3CO_3^- + 4\ H^+$ (-14.0457 log K) reaction in DATA0.FM2; [e] values confirmed in file "4b2b. ThHA Stern fit applied to WIPP in 33 mM MgCl2 1xEDTA.pqo" (see Table 7).
Note: Log β values use activities for H^+ and OH^- and molalities for all other species.

Table 3. Th(IV)-Ca-Mg-humic acid reaction database

Reaction	Log β (0.1 M) (Stern et al. 2014)	Log K (0 M) Fit for DATA0.FM2	Log β (0.1 M) for DATA0.FM2
$Hs^- + H^+ = HsH(aq)$	4.3	4.3	4.3
$Th^{4+} + Hs^- = ThHs^{3+}$	23.19[a] (pH 8.84) 23.80[a] (pH 9.22)	23.45[b,c] (pH 8.84) 24.52[b,c] (pH 9.22)	21.74[c] (pH 8.84) 22.81[c] (pH 9.22) 22.89[c] (pH 9.26)
$Ca^{2+} + Hs^- = CaHs^+$ $Mg^{2+} + Hs^- = MgHs^+$	3.0[d]	3.35[e]	3.0

[a] Stern et al. (2014, Fig. 3a)
[b] Fit to DATA0.FM2 database and to partitioning observed in Stern et al. (2014); for these log K values the activity coefficient of each Hs species (Hs^-, HsH, $CaHs^+$, $MgHs^+$, and $ThHs^{3+}$) is fixed at one in the model
[c] File "3b. ThHA Stern fit at low pCO2 to FMT davies.pqo" listed in Table 4
[d] Based on Lead et al. (1994), Laszak and Choppin (2001), and Lu and Allen (2002)
[e] Adjusted to achieve a log β value of 3.0 at 0.1 M ionic strength (Section 4.2.1)

4.2.1 Humic Complexation of H$^+$, Ca^{2+}, and Mg^{2+}

The stability constants for the humic complexation reactions in Table 3 are either selected from the literature or derived. The complexation of H^+ and the alkaline earths are selected.

For the protonation of the humic complexation site, $\log \beta_{1:H^+}$ is set at 4.3 as in the Stern et al. (2014) model. This value implies that the site becomes largely deprotonated above pH 4.3. Because WIPP brines are alkaline and there is little affinity of the modeled humic site for protons in alkaline waters, this

reaction has a negligible effect on the dominant speciation of humic sites in the WIPP calculations. Therefore, no adjustment to the log $\beta_{1:H^+}$ value is made.

For the humic complexation of Ca^{2+} and Mg^{2+}, the log value for $\beta_{1:Ca^{2+}}$ was conservatively set to 2.0 in the original WIPP model (DOE 1996, SOTERM.6.3.3.1). That value was based on experimental data on humic and fulvic acids. In this work, the value is increased to 3.0 but is still likely conservative based on studies over a broad range of pH, ionic strength, and concentrations of Ca^{2+} (Lead et al. 1994, Fig. 4b; Laszak and Choppin 2001, Fig. 4; Lu and Allen 2002, Table 5). At pcH 9, log $\beta_{1:Ca^{2+}}$ is found to be in the range of 3.3 to 4.3 for Aldrich humic acid (Laszak and Choppin 2001, Table 3). As the concentration of Ca^{2+} increases from 10^{-8} M in a 0.1 M NaCl solution (Laszak and Choppin 2001) to 0.033 M in a 0.033 M $CaCl_2$ solution (Lead et al. 1994), the log $\beta_{1:Ca^{2+}}$ is found to remain above 3.0 (approximately 3.4). Lu and Allen (2002) show a strong competitive effect of Ca^{2+} and Cu^{2+} to at least 0.001 M Ca (pH 6-7). Compared to $\beta_{1:Th^{4+}}$ the pH dependence of $\beta_{1:Ca^{2+}}$ is weak (Laszak and Choppin 2001; Lu and Allen 2002). For this work the simplifying conservative assumption is that log $\beta_{1:Ca^{2+}}$ is 3.0 for all humic complexation of Ca^{2+} regardless of pH. This value is also used for Mg^{2+}-humic complexation due to the similar humic complexation behavior of Mg^{2+} (Lead et al. 1994). The value of 3.35 for the log K at 0 M ionic strength gives a log $\beta_{1:Ca^{2+}}$ of 3.0 at 0.1 M ionic strength. This is a direct result of the log activity coefficient for Ca^{2+} at 0.1 M ionic strength in the simulations being -0.35 while the log activity coefficients of Hs^- and $CaHs^+$ are held at zero.

4.2.2 Th(IV)-Humic Complexation

The $ThHs^{3+}$ species in Table 3 represents the humic-bound actinide species AnHs of Eq. 2. The associated stability constant is a function of pH. The log K values at pH 8.84 and 9.22 (the pH values of WIPP brines in Table 1) were derived using the four-step process described below. The simulations performed for the derivation are listed in Table 4 along with their associated input/output files and post-processing files.

Table 4. Phreeqcl input/output files and Excel spreadsheets used in the derivation of the Th(IV)-humic log K values for DATA0.FM2 (/nfs/data/CVSLIB/WIPP_EXTERNAL/ap167/Files).

Simulation	Files
Step 1 – Th(IV)-humic-EDTA-CO_2-H_2O model of Stern et al. (2014)	1. ThHA Stern complexation reproduction Davies pH 7-8.pqi 1. ThHA Stern complexation reproduction Davies pH 7-8.pqo 1ThHAsternOUTdavies-pH78.xls 1. ThHAstern reproduction Davies pH7-8.xlsx
Step 1 – Same except $CO_2(aq)$ substituted for $CO_2(g)$ in the Stern et al. (2014) reaction for $Th(OH)_3CO_3^-$	1d. ThHA Stern reproduction Davies pH 7-8 modified.pqi 1d. ThHA Stern reproduction Davies pH 7-8 modified.pqo 1dThHAsternOUTdavies-pH78mod.xls 1d. ThHAstern reproduction Davies pH7-8mod.xlsx
Steps 2 and 3 – Th(IV)-humic-EDTA-H_2O model of Stern et al. (2014)	1b. ThHA Stern reproduction Davies NO CO2.pqi 1b. ThHA Stern reproduction Davies NO CO2.pqo 1bThHAsternOUTdaviesNoCO2.xls 1b. ThHAstern reproduction Davies NO CO2.xlsx
Step 4 – Th(IV)-humic-EDTA-H_2O model fitted to DATA0.FM2 database	3b. ThHA Stern fit at low pCO2 to FMT davies.pqi 3b. ThHA Stern fit at low pCO2 to FMT davies.pqo 3bThHAsternFitLowpCO2OUTdavies.xls 3b. ThHAstern fit Davies NO CO2.xlsx

Step 1 – Reproduce the Th(IV)-humic-EDTA-CO_2-H_2O system of Stern et al. (2014)

17

PhreeqcI was used to reproduce the system presented in Stern et al. (2014) over a pH range of 5 to 8. The Stern et al. (2014) system contains 5×10^{-5} M EDTA, 5×10^{-5} M humic acid sites, 0.1 M NaCl, and an atmospheric partial pressure of $CO_2(g)$. The humic acid used in the study was derived from Elliot soil (EHA) and Pakoekee Peat (PHA). The Stern et al. (2014) reaction data (Table 2) were used without modification.

The results shown in Figure 1 approximately reproduce the results of Stern et al. (2014, Fig. 5). A noticeable difference, however, is that the $Th(OH)_3CO_3^-$ species is overpredicted using the published reactions. A better match for all species to the results of the Stern et al. (2014, Fig. 5) model is obtained by changing the $CO_2(g)$ reactant in the $Th(OH)_3CO_3^-$ reaction to $CO_2(aq)$. It is highly likely that either the $CO_2(g)$ reactant in the stated reaction should be $CO_2(aq)$ or the wrong log β is shown for the stated reaction. Changing the reactant to $CO_2(aq)$ provides the results shown in Figure 2.
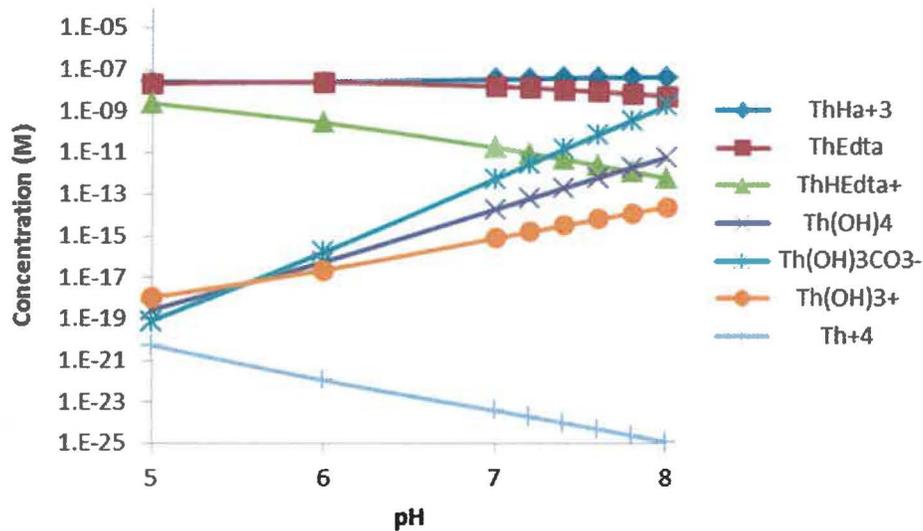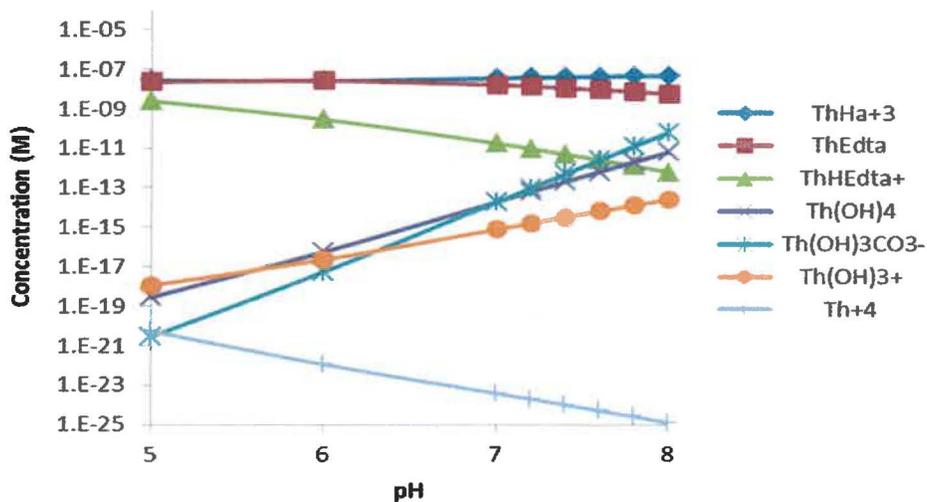

Figure 1. Reproduction of Stern et al. (2014) model

Figure 2. Stern et al. (2014) model using $CO_2(aq)$ as reactant in $Th(OH)_3CO_3^-$ reaction

Step 2 – Remove CO₂ from the Stern et al. (2014) system

The partial pressure of $CO_2(g)$ was removed from the Stern et al. (2014) system. This step was taken to eliminate the $Th(OH)_3CO_3^-$ issue identified in step 1 and to determine the extent of Th(IV)-humic complexation that would be predicted by the Stern et al. (2014) model in the absence of $CO_2(g)$. In this simulation, the pH range was extended to 9.22 to include pH values for equilibrated WIPP brines (Table 1). The results are plotted in Figure 3.
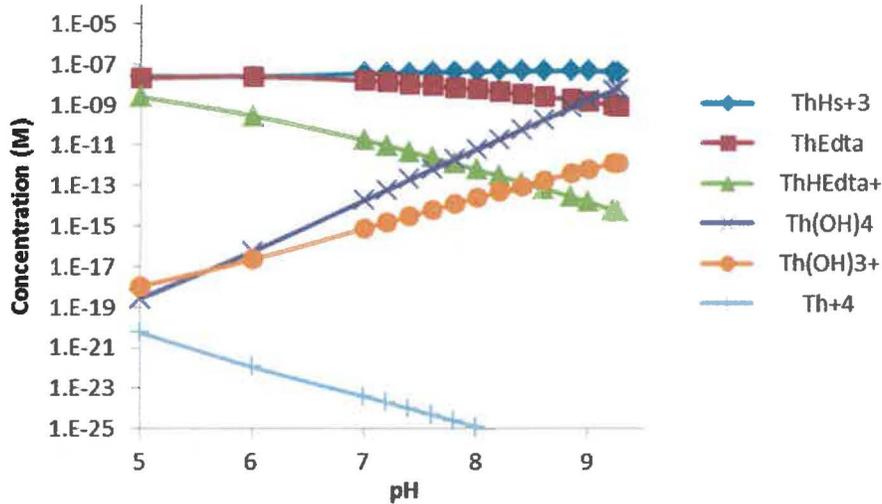
Figure 3. Speciation of the of Stern et al. (2014) system in the absence of CO_2

Step 3 – Calculate the percentage of Th(IV) complexed with humics over pH range

The percentage Th(IV) complexed with humics was calculated from the model results in step 2 over the pH range simulated. It is shown by the top curve plotted in Figure 4. This step provided the endpoint values for step 4 calibration.

Figure 4. Distribution of Th(IV) for the Th(IV)-humic-EDTA-H₂O system of Stern et al. (2014)

Step 4 – Derive log $K_{1:Th^{4+}}$ values for DATA0.FM2 database

In step 4, the Th(IV)-humic-EDTA-H_2O system of Stern et al. (2014) (i.e., the system produced in step 2) was reproduced using the DATA0.FM2 database in Table 2 and the humic complexation reactions in Table 3. The log K values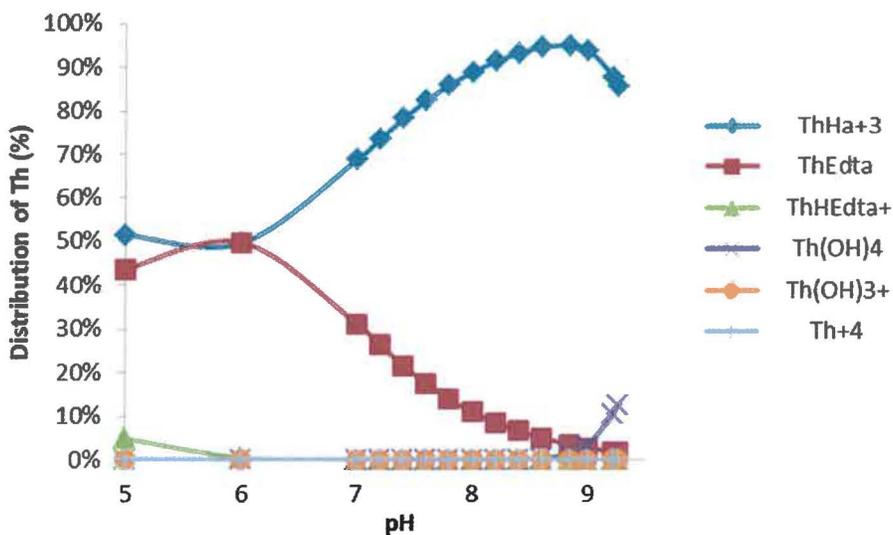 for the $ThHs^{3+}$ complexation reaction were adjusted at each pH until they provided Th(IV)-humic complexation that matched the percentage of Th(IV) complexed by humics calculated in step 3. This fitted model was not extended below pH 7 because the DATA0.FM2 database does not include Th(IV) hydrolysis products $Th(OH)_3^+$, $Th(OH)_2^{2+}$, and $ThOH^{3+}$, which could become important below pH 7. The fitted log K values for $ThHs^{3+}$ in the DATA0.FM2 database use the activity (not concentration) of Th^{4+}. These values are converted to log $\beta_{1:Th^{4+}}$ values in Table 3 by effectively multiplying the fitted K value by the Th^{4+} activity coefficient and taking the logarithm.

The trend of log $\beta_{1:Th^{4+}}$ as a function of pH is shown in Figure 5. Similar trends are observed for Th(IV) in Stern et al. (2014) and for Th(IV) and U(IV) in other humic complexation studies (Reiller et al. 2003; Warwick et al. 2005; Reiller et al. 2008).
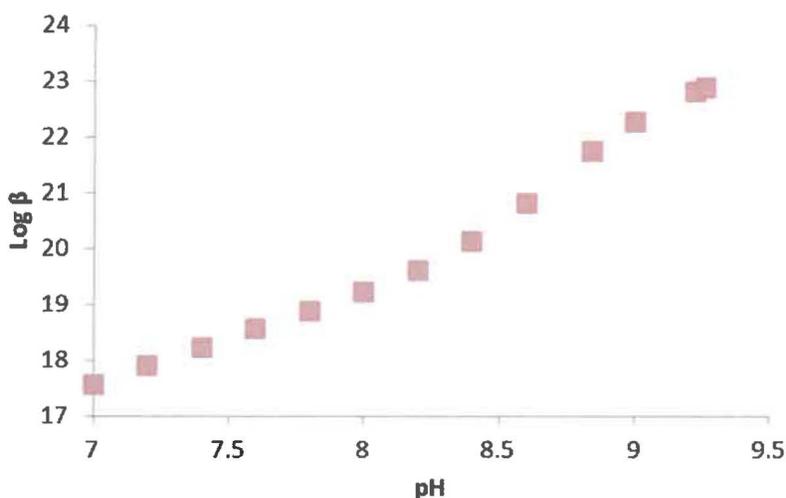

Figure 5. Log $\beta_{1:Th^{4+}}$ values calculated for DATA0.FM2 to simulate the Th(IV)-humic-EDTA-H_2O system of Stern et al. (2014)

4.2.3 U(IV)-Humic Complexation

Complexation of U(IV) with Belgian Boom Clay humic acid (BCHA) and Aldrich humic acid (AHA) was studied at pH values from 6 to 9 (Warwick et al. 2005). These experiments were performed in a 0.2 M Na_2SO_4 solution free of carbonate. Plots of the measured U(IV)-humic acid stability constants in these studies show a highly linear, increasing trend with pH for each humic acid (Warwick et al. 2005, Fig. 2 and 3; Reiller et al. 2008, Fig. 2).

The Warwick et al. (2005) data were used by Reiller et al. (2008) to develop a set of stability constants consistent with the hydrolysis data of Neck and Kim (2001). The hydrolysis reactions are shown in Table 5. In alkaline water, the $U(OH)_4(aq)$ species dominates. The log $\beta_{1:U^{4+}}$ values calculated by Reiller et al. (2008) from the Warwick et al. (2005) data are plotted in Figure 6. Linear regressions corresponding to these constants are presented in Table 6 and file "Reiller 2008 correction of Warwick.xlsx".

20

The $\log \beta_{1:U^{4+}}$ values in Figure 6 are clearly much higher than the $\log \beta_{1:Th^{4+}}$ values in Figure 5. This does not indicate, however, that U^{4+} has a much higher affinity for humic complexation sites than Th^{4+}. $U(OH)_4(aq)$ is more stable than $Th(OH)_4(aq)$, as indicated by the respective formation constants, -10.0 (Table 5) and -17.5 (Table 2). Consequently, in a simple alkaline solution having equal aqueous concentrations of Th(IV) and U(IV), the concentration of U^{4+} will be much lower than the concentration of Th^{4+}. Thus, the lower concentration of U^{4+} at a given alkaline pH will largely compensate for the higher $\log \beta_{1:U^{4+}}$ value to produce UHs^{3+} concentrations and U(IV) proportionality coefficients H that are comparable to those of $ThHs^{3+}$. This is demonstrated in Section 5.3.

Table 5. U(IV) hydrolysis reactions of Reiller et al. (2008, Table 2)

Reaction	Log K (0 M)	Log β (0.101 M)
$U^{4+} + 4\ H_2O = U(OH)_4(aq) + 4\ H^+$	-10.0	-11.3
$U^{4+} + 3\ H_2O = U(OH)_3^+ + 3\ H^+$	-4.7	-6.0
$U^{4+} + 2\ H_2O = U(OH)_2^{2+} + 2\ H^+$	-1.1	-2.2
$U^{4+} + H_2O = UOH^{3+} + H^+$	-0.4	-1.0

Table 6. Linear regression of U(IV)-humic stability constants in Reiller et al. (2008) model

Reaction	Humic Material	Log β [a]	Coefficient of Determination	Range of Mean pH
$U^{4+} + Hs^- = UHs^{3+}$	BCHA	4.340*pH – 7.674	0.9923	6.90 – 8.15
	AHA	3.972*pH – 6.255	1.0000	6.43 – 8.52

[a] Ionic strength for the reported stability constants is not specified (Reiller et al. 2008).
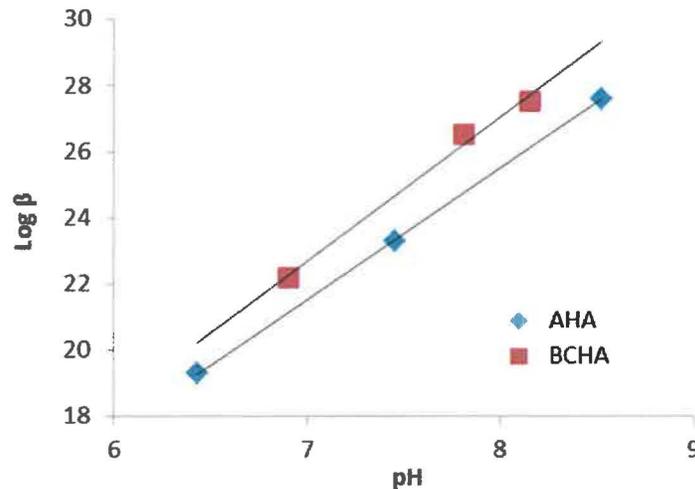
Figure 6. Log $\beta_{1:U^{4+}}$ values consistent with hydrolysis reactions of Neck and Kim (2001) (Reiller et al. 2008, Table 5)

4.2.4 Pu(IV)-Humic Complexation

Pu(IV) complexation with Leonardite humic acid was recently studied over a pH range of 4 to 6.5 by Zimmerman et al. (2014). In the study Pu(IV)-humic complexation is modeled using a charge neutralization model. H^+ is included in the Pu(IV)-humic complexation reaction such that the modeled complex is $Pu(OH)_2Hs^+$. Zimmerman et al. (2014) also studied humic complexation of Th(IV) and modeled it using an analogous complex, $Th(OH)_2Hs^+$. Although the Zimmerman et al. (2014) model was reproduced in the current study using PhreeqcI, it was not useful for WIPP conditions because it applies to acidic waters. Extrapolation of the Zimmerman et al. (2014) model to pH 9 could not be justified.

5 MODEL APPLICATION

In this section the An(IV)-humic complexation model developed in Section 4 is used to simulate complexation in WIPP-related waters. In Section 5.1, complexation is simulated in a 0.033 M $MgCl_2$ solution to examine the effect of a moderate concentration of Mg^{2+} on An(IV)-humic complexation in a solution of 0.1 M ionic strength.

WIPP brines equilibrated with MgO (Table 1) have much higher concentrations of Mg^{2+} and therefore have ionic strengths that far exceed the range of the PhreeqcI ion activity model. For WIPP brines, the Domski and Xiong (2015) calculations (Table 1) are used as input to calculate An(IV)-humic complexation. The Domski and Xiong (2015) calculations were performed using EQ3/6, Version 8.0a (Wolery and Jarek 2003; Wolery 2008; Wolery et al. 2010; Xiong 2011) and the thermodynamic database DATA0.FM2 (Domski 2015) and do not include the presence of humic colloids. The Domski and Xiong (2015) calculations are used in Section 5.2 for Th(IV)-humic complexation in WIPP brines and in Section 5.3 for U(IV)-humic complexation in WIPP brines.

The calculations in Sections 5.2 and 5.3 were performed using Microsoft Excel 2010 and PTC Mathcad Prime 3.0, a commercial mathematical software tool. The Mathcad files are saved in PDF format for documentation so that they can be read using Adobe Acrobat. It is clear from these PDF files exactly what algebraic calculations were performed. The calculated values shown in these files are easily checked by reading the file and using a hand calculator, so there is no need to include the Mathcad MCDX files in the data record. The input/output and post-processing files associated with the various model applications are listed in Table 7.

Table 7. Input/output and post-processing files used in the model applications
(/nfs/data/CVSLIB/WIPP_EXTERNAL/ap167/Files).

Simulation	Files
Section 5.1 – Th(IV)-humic complexation in a "dilute" WIPP simulant (0.033 M $MgCl_2$ solution)	4b2b. ThHA Stern fit applied to WIPP in 33 mM MgCl2 1xEDTA.pqi 4b2b. ThHA Stern fit applied to WIPP in 33 mM MgCl2 1xEDTA.pqo 4b2b. ThHA Stern fit applied to WIPP in 33 mM MgCl2 1xEDTA.xlsx
Section 5.2 – Th(IV)-humic complexation in WIPP brines	5. Th-CaMg-HA Stern fitted to FMT (1xMin) r1.mcdx.pdf 5b. Th-CaMg-HA Stern fitted to FMT 5xMinVol r1.mcdx.pdf
Section 5.3 – U(IV)-humic complexation in WIPP brines	3. U(IV)_HA beta data reduction 1x r1.mcdx.pdf 3. U(IV)_HA beta data reduction 5x r1.mcdx.pdf 5. U(IV)-CaMg-HA Warwick 1x r1.mcdx.pdf 5. U(IV)-CaMg-HA Warwick 5x r1.mcdx.pdf Reiller 2008 correction of Warwick.xlsx

5.1 Th(IV)-Humic Complexation in a 0.033 M $MgCl_2$ Solution

A 0.033 M $MgCl_2$ solution is used for this simulation because it has an ionic strength of 0.1 M and presents a fairly high concentration of Mg^{2+} to compete with Th^{4+} for humic complexation sites. The ionic strength is consistent with the ionic strengths associated with the conditional stability constants selected and derived in Section 4. In this simulation, apart from the major electrolytes, WIPP conditions (Section 3) are imposed. The total humic acid concentration is set to 1.1×10^{-5} M and the partial pressure of $CO_2(g)$ is set to 5.84×10^{-7} atm (Table 1). As in the GWB (1 × Min) brine of Table 1, the total Th(IV) concentration is set to 4.78×10^{-8} M, and the EDTA concentration is set to 7.40×10^{-5} M. The pH is varied from 7 to 9.3 to assess Th(IV)-humic complexation in this system as a function of pH. The log $\beta_{1:Th^{4+}}$ values used in the simulations for the different pH values correspond to the values shown in Figure 5.

Results are shown in Figure 7 through Figure 9. Over 95% of the humic complexation sites are occupied by Mg^{2+} over the entire pH range simulated. As the concentration of $Th(OH)_4(aq)$ rises and the concentration of Th^{4+} falls with increasing pH (Figure 7), the fraction of Th(IV) that is humic-bound falls from about 99% to less than 10% (Figure 8). The corresponding proportionality coefficient H versus pH is shown in Figure 9. Though the stability constant $\beta_{1:Th^{4+}}$ increases with pH, the proportionality coefficient H decreases with pH. The reason for this is that as pH increases the concentration of Th^{4+} decreases more rapidly than $\beta_{1:Th^{4+}}$ increases.
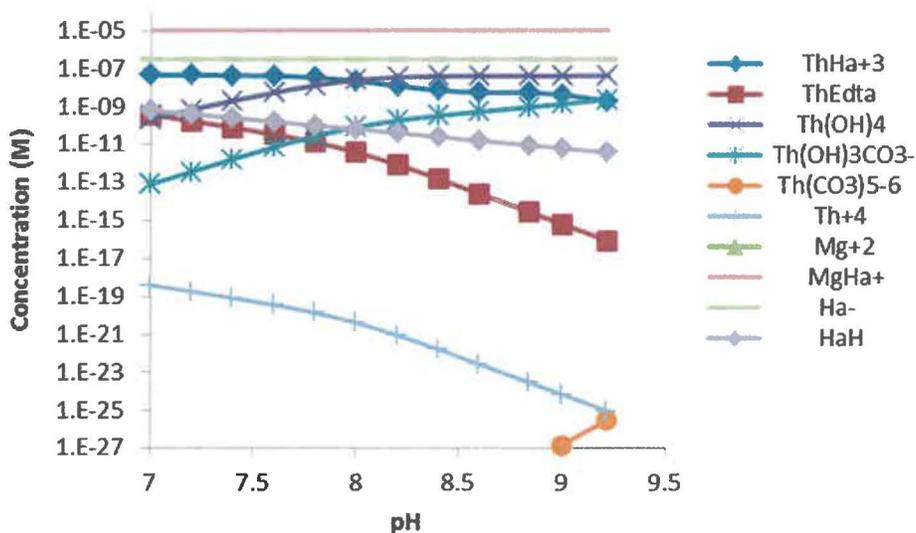
Figure 7. Predicted speciation in a 0.033 M MgCl$_2$ solution, 4.78×10^{-8} M Th(IV), 1.1×10^{-5} M Hs, 5.84×10^{-7} atm CO$_2$, and 7.40×10^{-5} M EDTA
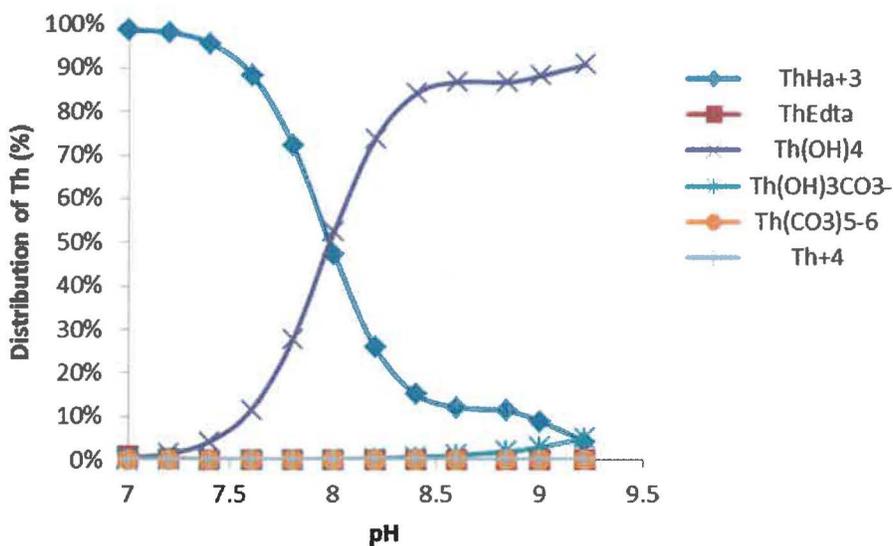
Figure 8. Predicted Th(IV) distribution in a 0.033 M MgCl$_2$ solution, 4.78×10^{-8} M Th(IV), 1.1×10^{-5} M Hs, 5.84×10^{-7} atm CO$_2$, and 7.40×10^{-5} M EDTA

23
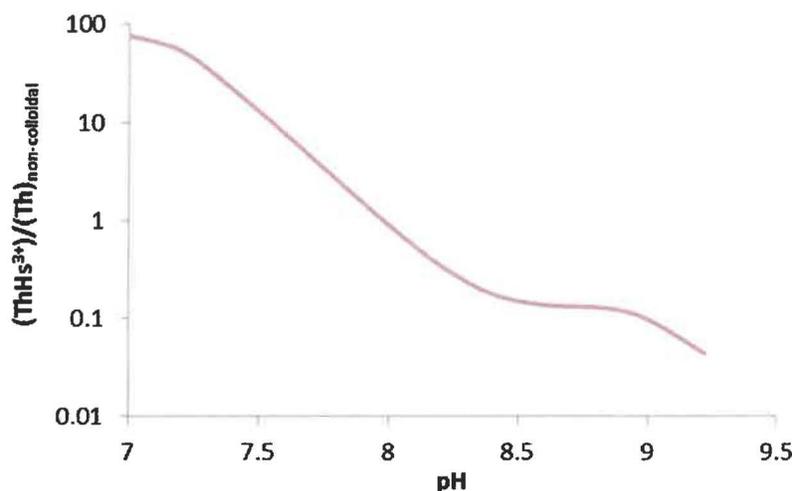
Figure 9. Predicted proportionality coefficient H in a 0.033 M $MgCl_2$ solution, 4.78×10^{-8} M Th(IV), 1.1×10^{-5} M Hs, 5.84×10^{-7} atm CO_2, and 7.40×10^{-5} M EDTA

5.2 Th(IV)-Humic Complexation in WIPP Brines

WIPP brines have an ionic strength around 6 M (Table 1). These brines cannot be simulated using the PhreeqcI model developed in the previous section because the ionic strength far exceeds the range of the ion activity model. In its place, the EQ3/6 Pitzer ion interaction model can be used (e.g., Domski and Xiong 2015). However, this is not necessary because the calculations of the Domski and Xiong (2015) model, shown in Table 1, can be directly used to predict Th(IV)-humic complexation in equilibrated WIPP brines.

The calculations of Domski and Xiong (2015) assume that a mineral phase (hydrous, amorphous ThO_2) controls the solubility of Th(IV). This implies that the free Th^{4+} concentration will not be affected by the addition of humic colloids. Thus, the fraction of Th(IV) complexed by aqueous humic substances in equilibrated WIPP brines can be calculated directly from the equations in Section 4.1, the concentrations in Table 1, and the stability constants in Table 3.

Using the stability constants in Table 3 for WIPP brines requires the additional assumption that these constants are adequate to use without adjustment for WIPP brines. Laboratory measurements indicate that as the ionic strength of a NaCl solution increases from 0.1 M to 5 M, log $\beta_{1:Ca^{2+}}$ decreases (Laszak and Choppin 2001). It is expected that log $\beta_{1:Th^{4+}}$ will also decrease as ionic strength increases. Thus, combined with a log $\beta_{1:Ca^{2+}}$ of 3.0, which is shown to be low compared to measurements at high pH and high ionic strength (Laszak and Choppin 2001, Fig. 4), the assumption that the stability constants in Table 3 can be used for WIPP brines is expected to result in conservative overestimation of Th(IV)-humic complexation in WIPP brines.

Table 8 summarizes the calculated speciation for each of the brines. The concentrations of Hs^- and AnHs are calculated directly from Eq. 4 and 5. Concentrations of humic-bound Th(IV) in WIPP brines are calculated to be less than 1% of concentrations calculated in the original model. More than 99% of the humic complexation sites are predicted to be occupied by Ca and Mg. The very low concentration of Th^{4+} ($<10^{-24}$ M) at pH ~9 combined with the low concentration of Hs^- ($<10^{-7}$ M) severely limits the humic-bound Th(IV) concentration.

24

The proportionality coefficients, calculated from Eq. 1, are shown in Table 9. They range from 0.0006 to 0.0071. These values are far lower than the legacy value of 6.3.

Table 8. Predicted concentrations (M) in Th(IV)-Ca-Mg-Hs system for WIPP PA

Parameter	GWB (1 × Min)	GWB (5 × Min)	ERDA-6 (1 × Min)	ERDA-6 (5 × Min)
(An)[a]	4.78×10^{-8}	4.80×10^{-8}	5.46×10^{-8}	5.54×10^{-8}
(An^{m+})[a]	1.16×10^{-25}	1.03×10^{-25}	1.12×10^{-26}	7.28×10^{-27}
(Hs$_{tot}$)[b]	1.10×10^{-5}	1.10×10^{-5}	1.10×10^{-5}	1.10×10^{-5}
(Ca^{2+})[c]	0.0280	0.0289	0.0160	0.0160
(Mg^{2+})[c]	0.282	0.276	0.0506	0.0419
(Hs$^-$)	3.54×10^{-8}	3.59×10^{-8}	1.63×10^{-7}	1.87×10^{-7}
(CaHs)+(MgHs)	1.096×10^{-5}	1.096×10^{-5}	1.084×10^{-5}	1.081×10^{-5}
(AnHs)	3.26×10^{-11}	2.78×10^{-11}	3.83×10^{-10}	3.93×10^{-10}

[a] Domski and Xiong (2015)

[b] Assumed (Section 3)

[c] Molarity calculated from Table 1 (free cation molality multiplied by solution density)

Table 9. Proportionality coefficients calculated for Th(IV)

Humic Material	GWB	ERDA-6	Source
Seawater	6.3	6.3	DOE (1996)
EHA and PHA	0.00068 (1 x Min[a]) 0.00058 (5 x Min)	0.0070 (1 x Min) 0.0071 (5 x Min)	This work

[a] minimum brine volume for a DBR from the repository

5.3 U(IV)-Humic Complexation in WIPP Brines

The U(IV)-humic complexation model of Reiller et al. (2008), described in Section 4.2.3, is used here to simulate U(IV)-humic complexation in the equilibrated WIPP brines of Table 1. These simulations use experimental data from Warwick et al. (2005) and the hydrolysis reactions of Neck and Kim (2001). The reactions are listed in Table 5 and Table 6.

As in the case of the calculation of Th(IV)-humic complexation in WIPP brines (Section 5.2), the PhreeqcI model of Section 5.1 could not be used because the ionic strength exceeds the range of the ion activity model. In the Section 5.2 calculation, the concentration of Th^{4+} was provided by simulations by Domski and Xiong (2015) that used a Pitzer ion interaction model to equilibrate the WIPP brines. Results of those simulations are shown in Table 1. Because those simulations do not include U(IV), the concentration of U^{4+} in each of the brines required calculation. This was done by assuming that the activity coefficients of U^{4+} in each brine are equal to those of Th^{4+} in the Domski and Xiong (2015) calculations. The concentrations of U^{4+} could then be calculated from the model reactions (Table 5 and Table 6), the total dissolved concentration, and the pH values of the brines. The total dissolved concentration is assumed to be equal to the total Th(IV) concentrations in Table 1. The resulting U^{4+} concentrations range from 2.69×10^{-34} M to 3.87×10^{-33} M, which are much lower than the Th^{4+} concentrations (Table 1). These calculations are documented in "3. U(IV)_HA beta data reduction 1x r1.mcdx.pdf" and "3. U(IV)_HA beta data reduction 5x r1.mcdx.pdf".

The remaining calculations are similar to the calculations in Section 5.2. Ca^{2+} and Mg^{2+} are added as indicated in Table 1, and either BCHA or AHA is added at a concentration of 1.10×10^{-5} M. The linear regressions in Table 6 are used to calculate $\beta_{1:U^{4+}}$ at the pH values of the brines. This is reasonable based

on the high linearity of $\log \beta_{1:U^{4+}}$ as a function of pH from 6 to 9 (Warwick et al. 2005, Fig. 2 and 3; Reiller et al. 2008, Fig. 2).

The simulations involving BCHA required an increase in the $\log \beta_{1:Ca^{2+}}$ value to 5.0. The $\log \beta_{1:Ca^{2+}}$ value of 3.0 selected in Section 4.2.1 is based on experimental data involving AHA only. As shown in Table 6 and Figure 6, BCHA has a much higher affinity for U^{4+} than AHA; therefore, BCHA should also have a much higher affinity for Ca^{2+} and Mg^{2+}. The linear regressions indicate that at pH 9 the $\log \beta_{1:U^{4+}}$ for BCHA is approximately 2 units higher than for AHA. The linear regression for BCHA may possibly overestimate the $\log \beta_{1:U^{4+}}$ value at pH 9; however, overestimation of $\log \beta_{1:U^{4+}}$ is conservative. Because this regression is used in this analysis, it is appropriate for the $\log \beta_{1:Ca^{2+}}$ value for BCHA to also be increased by 2 units relative to the value used for AHA.

The proportionality coefficients calculated in this analysis are summarized in Table 10. The associated calculations are documented in files "5. U(IV)-CaMg-HA Warwick 1x r1.mcdx.pdf" and "5. U(IV)-CaMg-HA Warwick 5x r1.mcdx.pdf". As in the case of the calculated proportionality coefficients for Th(IV) in Table 9, these coefficients are low to very low compared to the legacy value of 6.3.

Table 10. Proportionality coefficients calculated for U(IV)

Humic Material	GWB	ERDA-6	Source
Seawater	6.3	6.3	DOE (1996)
BCHA	0.00021 (1 x Min[a])	0.0083 (1 x Min)	This work
	0.00018 (5 x Min)	0.0104 (5 x Min)	
AHA	0.00031 (1 x Min)	0.0087 (1 x Min)	This work
	0.00026 (5 x Min)	0.0106 (5 x Min)	

[a] minimum brine volume for a DBR from the repository

5.4 Recommendations for PHUMSIM and PHUMCIM for An(IV)

The proportionality coefficients calculated in this report for WIPP brines are plotted in Figure 10 for GWB and ERDA-6. Two of the six points for each brine are from the analysis of Th(IV) complexation with EHA and PHA (Table 9). The remaining points are from the analysis of U(IV) complexation with BCHA and AHA (Table 10).

As shown in Figure 10, the brine composition is highly important to the calculated proportionality coefficients. The PHUMCIM values for ERDA-6 are more than 10 times higher than the PHUMSIM values for GWB. The main reason for this is that the Mg^{2+} concentration is much lower in ERDA-6; therefore, Mg^{2+} competes much less for the available humic complexation sites in ERDA-6. As for the dilution of the brine (i.e., 1 × Min vs. 5 × Min), it makes little difference to the calculated PHUMSIM and PHUMCIM values.

Table 11 summarizes the recommended probability distributions for PHUMSIM and PHUMCIM. Broad log triangular distributions are recommended that are guided by the calculations but also provide a low likelihood for underestimation. The recommended minimum values are approximately half of the minimum values shown in Figure 10, and the recommended maximum values are approximately 10 (PHUMCIM) and 14 (PHUMSIM) times higher than the maximum values shown. Due to few data available and multiple assumptions in the calculations, a more quantitative approach for determining probability distributions cannot be justified and would not be consistent with the conservative approach accepted by the regulators in the original WIPP PA (Mariner and Sassani 2014).

The recommended maximum values for the distributions, while likely conservative, would provide the maximum humic colloid enhancement of An(IV) mobility in the WIPP PA. However, the impact of even

the maximum values on the WIPP PA will be small. Sampled values near the maximum values will have very low probability and will enhance An(IV) mobility by no more than 10% for ERDA-6 and no more than 1% for GWB. A quantitative analysis of how conservative these low-probability maximum values are is unwarranted because they will have little effect on total system performance assessment. If such an analysis were to be performed, it would need to consider that the calculated values for each brine (Figure 10) themselves have inherent conservative assumptions, including (1) that humic colloids are stable at a concentration of 2 mg L^{-1} in equilibrated WIPP brines despite evidence that they are likely unstable in the presence of MgO in these brines (Wall and Mathews 2005), and (2) that the stability constant for humic complexation of Ca^{2+} and Mg^{2+} is set to $10^{3.0}$ (and $10^{5.0}$ for BCHA) and not higher (Sections 4.2.1 and 5.3).

The legacy 6.3 value for PHUMSIM and PHUMCIM enhances the mobile concentration of An(IV) by 630% if no other types of An(IV) colloids are present. In contrast, the mode values recommended in Table 11 would enhance mobile concentrations by only 0.04% (GWB) and 1% (ERDA-6) relative to the non-colloidal An(IV) concentration. Thus, if no other types of An(IV) colloids are present (i.e., intrinsic, microbial, mineral fragment), the recommended PHUMSIM and PHUMCIM distributions would reduce the mobile An(IV) concentrations by 86% relative to the legacy calculations for the most likely sampled PHUMSIM and PHUMCIM values and by 86% (GWB) and 85% (ERDA-6) for the maximum PHUMSIM and PHUMCIM values sampled.
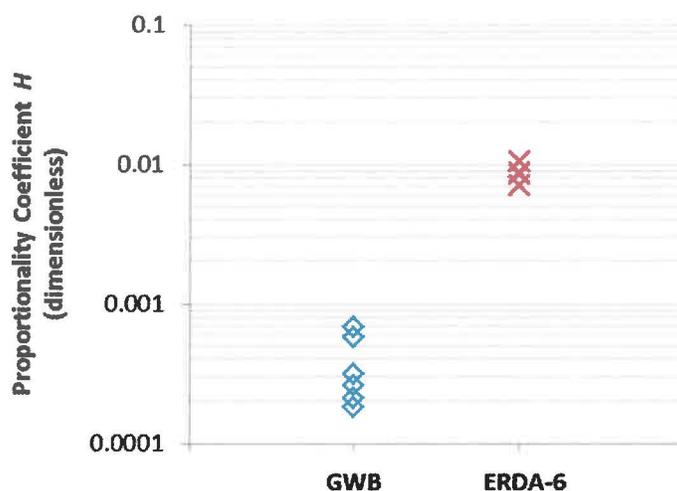

Figure 10. Plot of proportionality coefficients H calculated for Th(IV) and U(IV) in equilibrated WIPP brines

Table 11. Recommended distributions for PHUMSIM and PHUMCIM for An(IV)

Parameter	PHUMSIM	PHUMCIM
Distribution	Log triangular	Log triangular
Mode	0.0004	0.01
Minimum	0.0001	0.004
Maximum	0.01	0.1

6 CONCLUSIONS

In accordance with the Analysis Plan for the Evaluation of Humic-Actinide Complexation of WIPP Conditions, AP 167, Rev. 0 (Mariner 2014), an analysis of the humic complexation of An(IV) (i.e., tetravalent actinides) in WIPP brines was performed. Humic complexation data reported in the literature for Th(IV), U(IV), and Ca and for four different humic acids were used to develop a model to predict An(IV)-humic complexation in WIPP brines. Compared to legacy WIPP PA calculations, much lower An(IV)-humic complexation is predicted. All calculations in this report are stored on the CVS (Concurrent Versioning System) in /nfs/data/CVSLIB/WIPP_EXTERNAL/ap167/Files.

PHUMSIM and PHUMCIM are the proportionality coefficients in the WIPP PA model that represent the equilibrium aqueous ratios of the humic-bound actinide concentration to the non-colloidal actinide concentration for GWB and ERDA-6 brines, respectively. The legacy value for each of these parameters is 6.3 for actinides in the IV oxidation state. This value was established based on measurements of Th(IV) in different size fractions of ultra-filtered seawater (DOE 1996, SOTERM.6.3.3.1).

The ranges of the proportionality coefficients calculated for tetravalent actinides using the newly developed model are 0.00018 to 0.00068 for PHUMSIM and 0.0070 to 0.0106 for PHUMCIM (Table 9 and Table 10). These ranges are much lower than the legacy value of 6.3 primarily because equilibrated WIPP brines have higher pH (~9) and higher Mg concentrations. Mg^{2+} competes with An(IV) for humic complexation sites. The lower Mg^{2+} concentrations in ERDA-6 are the main reason the calculated PHUMCIM values are higher than the calculated PHUMSIM values.

The distributions recommended for the WIPP PA for tetravalent actinides are log triangular with minimum and maximum values of 0.0001 and 0.01 for PHUMSIM and 0.004 to 0.1 for PHUMCIM. The recommended modes are 0.0004 and 0.01, respectively. These distributions are conservative and will likely overestimate mean An(IV)-humic complexation for three reasons: (1) Mg-humic complexation is likely underestimated in the model (Section 4.2.1), (2) humic colloids appear to be unstable in WIPP brines in the presence of MgO (Section 2), and (3) the maximum values for the PHUMSIM and PHUMCIM distributions are conservative relative to the values calculated in this analysis (Figure 10). Regardless, the newly calculated PHUMSIM and PHUMCIM distributions, if adopted by the WIPP PA, would reduce humic-bound An(IV) to no more than 10% of non-colloidal aqueous An(IV) concentrations. This reduction implies that in the absence of significant concentrations of intrinsic, microbial, and mineral fragment colloids the total mobile An(IV) concentrations would be reduced by 85% to 86%.

7 REFERENCES

Baskaran, M., P. H. Santschi, G. Benoit and B. D. Honeyman (1992). "Scavenging of thorium isotopes by colloids in seawater of the Gulf of Mexico." Geochimica et Cosmochimica Acta **56**(9): 3375-3388.

Buffle, J. (1988). Complexation Reactions in Aquatic Systems. New York, New York, John Wiley & Sons.

DOE (1996). Title 40 CFR Part 191 Compliance Certification Application for the Waste Isolation Pilot Plant. DOE/CAO-1994-2184. U.S. Department of Energy, Carlsbad, NM.

DOE (2009). Title 40 CFR Part 191 Subparts B and C Compliance Recertification Application for the Waste Isolation Pilot Plant. DOE/WIPP 09 3424. U.S. Department of Energy Carlsbad, NM.

Domski, P. S. (2015). EQ3/6 Database Update: DATA0.FM2. Memo to SNL WIPP Records Center on October 27, 2015, ERMS 564914. Sandia National Laboratories, Carlsbad, New Mexico.

Domski, P. S. and Y. L. Xiong (2015). Prediction of Baseline Actinide Solubilities with an Updated EQ3/6 Thermodynamic Database (DATA0.FM2) in Response to EPA Completeness Comment 3-C-3 for CRA 2014. Sandia National Laboratories, Carlsbad, New Mexico. ERMS# 565032.

Enfield, C. G., G. Bengtsson and R. Lindqvist (1989). "Influence of Macromolecules on Chemical-Transport." Environmental Science & Technology **23**(10): 1278-1286.

Evans, N., P. Warwick, T. Lewis and N. Bryan (2011). "Influence of humic acid on the sorption of uranium(IV) to kaolin." Environmental Chemistry Letters **9**(1): 25-30.

Gaona, X., V. Montoya, E. Colas, M. Grive and L. Duro (2008). "Review of the complexation of tetravalent actinides by ISA and gluconate under alkaline to hyperalkaline conditions." Journal of Contaminant Hydrology **102**(3-4): 217-227.

Laszak, I. and G. R. Choppin (2001). "Interaction study between Ca2+ and humic acids in brine media." Radiochimica Acta **89**(10): 653-659.

Lead, J. R., J. Hamiltontaylor, N. Hesketh, M. N. Jones, A. E. Wilkinson and E. Tipping (1994). "A Comparative-Study of Proton and Alkaline-Earth Metal-Binding by Humic Substances." Analytica Chimica Acta **294**(3): 319-327.

Lu, Y. F. and H. E. Allen (2002). "Characterization of copper complexation with natural dissolved organic matter (DOM) - link to acidic moieties of DOM and competition by Ca and Mg." Water Research **36**(20): 5083-5101.

Mariner, P. E. (2014). Analysis Plan for the Evaluation of Humic-Actinide Complexation for WIPP Conditions. AP-167, Revision 0. Sandia National Laboratories, Carlsbad, New Mexico.

Mariner, P. E. and D. C. Sassani (2014). Analysis report for WIPP colloid model constraints and performance assessment parameters. SAND2014-1961. Sandia National Laboratories, Carlsbad, New Mexico.

Neck, V. and J. I. Kim (2001). "Solubility and hydrolysis of tetravalent actinides." Radiochimica Acta **89**: 1-16.

Parkhurst, D. L. (1995). User's Guide to PHREEQC--a Computer Program for Speciation, Reaction-Path, Advective-Transport, and Inverse Geochemical Calculations. Water-Resources Investigations Report 95-4227. U.S. Geological Survey,

Parkhurst, D. L. and C. A. J. Appelo (1999). User's Guide to PHREEQC (Version 2) – A computer program for speciation, batch-reaction, one-dimensional transport, and inverse geochemical calculations. Water-Resources Investigations Report 99-4259. U.S. Geological Survey,

Reiller, P., V. Moulin, F. Casanova and C. Dautel (2003). "On the study of Th(IV)-humic acid interactions by competition sorption studies with silica and determination of global interaction constants." Radiochimica Acta **91**(9): 513-524.

Reiller, P. E., N. D. M. Evans and G. Szabo (2008). "Complexation parameters for the actinides(IV)-humic acid system: a search for consistency and application to laboratory and field observations." Radiochimica Acta **96**(6): 345-358.

Stern, J. C., D. I. Foustoukos, J. E. Sonke and V. J. M. Salters (2014). "Humic acid complexation of Th, Hf and Zr in ligand competition experiments: Metal loading and pH effects." Chemical Geology **363**: 241-249.

USGS (2002). PhreeqcI – A Graphical User Interface to the Geochemical Model PHREEQC. USGS Fact Sheet FS-031-02. U.S. Geological Survey,

USGS (2005). PHREEQC (Version 2) – A Computer Program for Speciation, Batch-Reaction, One-Dimensional Transport, and Inverse Geochemical Calculations. Dec. 2, 2005.

Wall, N. A. and S. A. Mathews (2005). "Sustainability of humic acids in the presence of magnesium oxide." Applied Geochemistry **20**: 1704-1713.

Warwick, P., N. Evans, A. Hall, G. Walker and E. Steigleder (2005). "Stability constants of U(VI) and U(IV)-humic acid complexes." Journal of Radioanalytical and Nuclear Chemistry **266**(2): 179-190.

Wolery, T. W. (2008). Analysis plan for EQ3/6 analytical studies. AP-140, Rev. 0. Sandia National Laboratories, Carlsbad, New Mexico. ERMS 548930.

Wolery, T. W. and R. L. Jarek (2003). Software User's Manual EQ3/6, Version 8.0. Civilian Radioactive Waste Management System Management & Operations, Albuquerque, New Mexico.

Wolery, T. W., Y. L. Xiong and J. J. Long (2010). Verification and validation plan/validation document for EQ3/6 version 8.0a for actinide chemistry, document version 8.10. Sandia National Laboratories, Carlsbad, New Mexico. ERMS 550239.

Xiong, Y. L. (2011). WIPP verification and validation plan/validation document for EQ3/6 version 8.0a for actinide chemistry, revision 1. Supersedes ERMS 550239. Sandia National Laboratories, Carlsbad, New Mexico. ERMS 555358.

Zimmerman, T., M. Zavarin and B. A. Powell (2014). "Influence of humic acid on plutonium sorption to gibbsite: Determination of Pu-humic acid complexation constants and ternary sorption studies." Radiochimica Acta **102**(7): 629-643.